Chapter 4

Computational Models for the Study of Protein Aggregation

Nguyen Truong Co, Mai Suan Li, and Pawel Krupa

Abstract

Protein aggregation has been studied by many groups around the world for many years because it can be the cause of a number of neurodegenerative diseases that have no effective treatment. Obtaining the structure of related fibrils and toxic oligomers, as well as describing the pathways and main factors that govern the self-organization process, is of paramount importance, but it is also very difficult. To solve this problem, experimental and computational methods are often combined to get the most out of each method. The effectiveness of the computational approach largely depends on the construction of a reasonable molecular model. Here we discussed different versions of the four most popular all-atom force fields AMBER, CHARMM, GROMOS, and OPLS, which have been developed for folded and intrinsically disordered proteins, or both. Continuous and discrete coarse-grained models, which were mainly used to study the kinetics of aggregation, are also summarized.

Key words Protein aggregation, Coarse-grained model, Lattice model, AMBER, CHARMM, GROMOS, OPLS

1 Introduction

After synthesis in the ribosome, the protein can fold into a native state and is likely to become functional. However, under the influence of various factors, such as changes in the translation rate of codons, sequence, crowded environment, it can aggregate (Fig. 1), which can cause a number of neurodegenerative diseases [1]. Therefore, problem of protein aggregation has attracted the attention of many researchers in recent decades. Appearance of plaques from amyloid beta (Aβ) peptides and tau-protein in the brain is considered as a hallmark of Alzheimer's disease [2], while accumulation of α-synuclein is believed to cause Parkinson's disease [3]. In total, there are about 20 different neurodegenerative diseases associated with the self-assembly of various proteins, although fibrillar structures are applicable in some cases.

The study of protein aggregation includes the determination of the structure of aggregates and mechanisms of their formation. Depending on the conditions, the aggregate can be amorphous

Mai Suan Li et al. (eds.), *Computer Simulations of Aggregation of Proteins and Peptides*, Methods in Molecular Biology, vol. 2340, https://doi.org/10.1007/978-1-0716-1546-1_4,

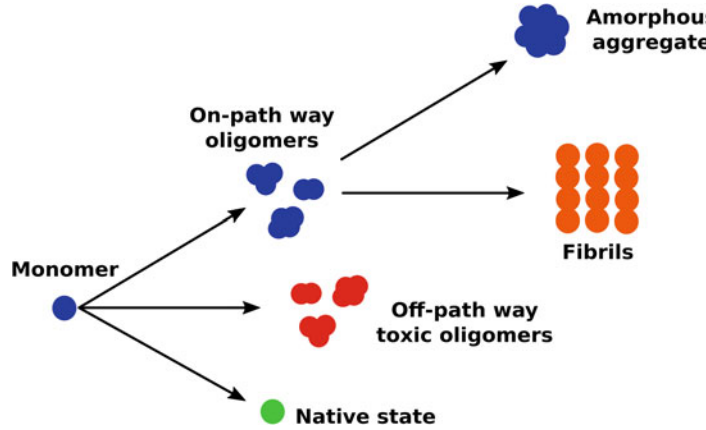

Fig. 1 Schematic graph showing that a protein can either fold into its native state in order to be functional or misfold to aggregate. There are three possible scenarios for aggregation: the formation of toxic off-pathway oligomers, amorphous aggregate, and fibrillar structure through on-pathway oligomers

(e.g., at a high concentration of metal ions) or fibrillar with a cross-beta structure, as shown by experiment using solid state NMR, solution NM, and cryo-EM. It was previously thought that only fibrils are toxic to the nervous system, but recent experimental studies have revealed that off-pathway oligomers are also highly toxic [4] (Fig. 1). Therefore, it is necessary to determine the structure of oligomers, but because of their transient nature, experimental methods cannot solve this problem. In such a context, computational tools such as molecular dynamics simulations are helpful.

Amyloid fibril formation mechanism has been experimentally proven to follow the nucleation growth mechanism [5, 6], in which the augmentation of aggregation mass in time obeys the sigmoid curve (Fig. 2) and consists of three characteristic stages: the lag phase, elongation or growth phase, and equilibrium or saturation phase [1, 7]. The lag phase corresponds to the period, in which soluble monomers randomly form unstable oligomers, and its end is marked by the formation of a primary critical nucleus, which acts as a stable template into which other peptides are favorably incorporated and contribute to fibril elongation. In the elongation phase, formation of protofibrils from the template obeys the "dock-lock" mechanism [8]. The accumulation of fibril mass also benefits from the secondary nucleation, where available small fibrils catalyzes the formation of oligomers on their surface, resulting in the formation of β-sheet-rich species [9]. Finally, as soon as the balance between the attachment of monomers to mature fibrils and their detachment is reached, the system enters the saturation phase.

Protein folding has been known to be computationally challenging due to a rough free energy landscape, but the numerical

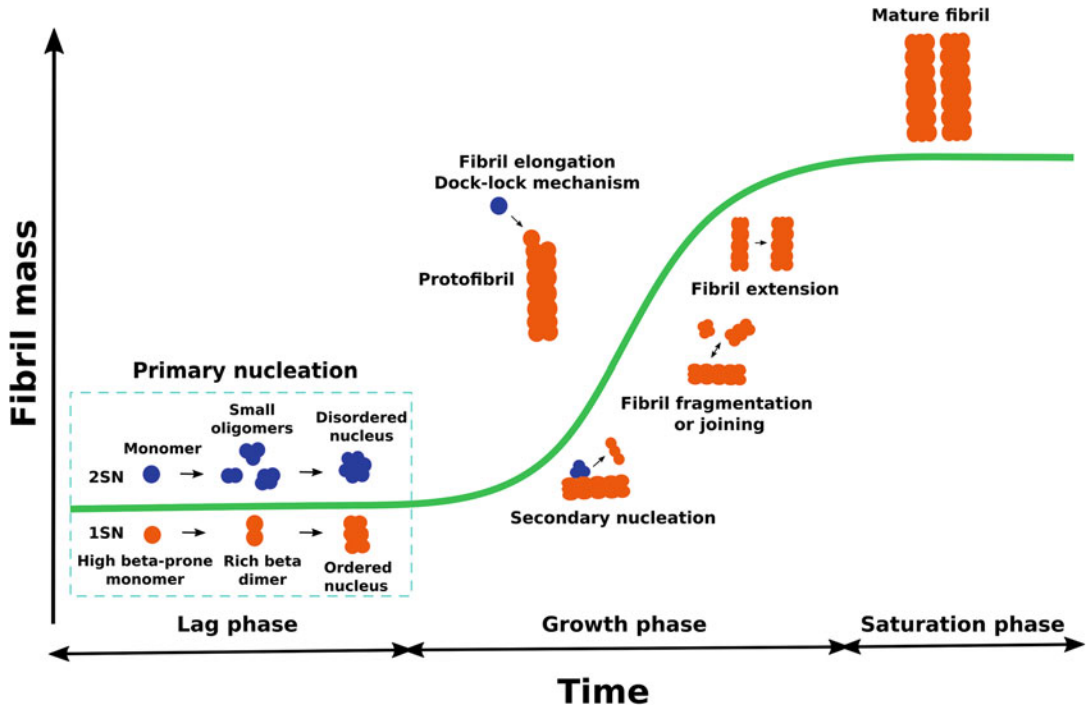

Fig. 2 Sigmoid kinetics of fibril formation process typically observed in the fluorescent experiment. Blue and orange colors represent species favoring disordered and ordered configurations, respectively. 1SN refers to one-step nucleation kinetics, in which highly amyloidogenic peptides can associate to form β-rich oligomers and then a critical nucleus. 2SN stands for two-step nucleation kinetics, in which poorly amyloidogenic peptides are first formed small amorphous oligomers, and then they evolve into a disordered stable critical nucleus, which gradually transforms its structure into a rich β-structure template

study of fibril formation is even more difficult because the fibril formation time (hour-day) is about four orders of magnitude longer than the folding time (μs–s). Therefore, all-atom molecular simulations are usually limited to the fibril formation of short amyloid peptides or the early stage of aggregation of longer proteins [10]. Coarse-grained models have often been used to study aggregation kinetics, but not to obtain a fibrillar structure unless they are hybridized with all-atom models.

There are many good reviews of coarse-grained [11] and all-atom force fields (FFs) [12, 13] and their application to study self-assembly of proteins. Therefore, our goal is to provide a short survey of the latest developments in this area, with a focus on coarse-grained models and our own contributions. Our review begins with a description of the main all-atom FFs developed for proteins that have a native state and intrinsically disordered proteins or both. We restrict ourselves to the results obtained using these FFs for the aggregation of amyloid proteins and peptides. Most of the current off- and on-lattice models and their application to the study of the thermodynamics and kinetics of oligomerization and

fibrillation will be briefly discussed. Future directions in the development of computational models for the study of the aggregation of biomolecules will be outlined.

2 Application of All-Atom Models to Study Protein Aggregation

All-atom FFs are the most natural choice to conduct theoretical studies of many biological phenomena involving proteins, nucleic acids, lipids, and sugars. Most of the FFs focusing on proteins are based on Anfinsen's dogma saying that at least for small globular proteins the native structure is determined only by the amino acid sequence [14]. However, the process of protein folding is so complicated that it is impossible to study all possible protein conformations [15]. Therefore, one should focus on a dominant folding pathway that leads to a native structure of proteins [16]. Although this is true for many proteins, it was found that protein aggregates and fibrils possess very stable and low-energy structures, which are kinetically preferable [17]. High stability of the fibrils is one of the reasons why diseases such as Alzheimer, Parkinson, or dementia with Lewy bodies are so difficult to treat [18, 19].

2.1 Typical FFs Used for Studies of Systems Involving Peptides or Proteins

The four most popular all-atom FFs used to study proteins are probably Amber [20], CHARMM [21], GROMOS [22], and OPLS [23]. Although technically only GROMOS and OPLS-UA are unified atom FFs, due to the fact that some hydrogen atoms are implicitly included in heavy-atom parameters with which they are covalently bound, other FFs are also using some tricks to constrain motion of some or all hydrogen atoms in order to speed up simulations, such as SHAKE [24], RATTLE [25], and SETTLE for rigid water molecule [26] algorithms. All of the mentioned FFs are non-polarizable and belong to first-generation FFs sharing very similar energy equation [27]. Therefore, the most significant differences between them are mostly due to various parameterization methods used to obtain parameters [28].

All of the popular all-atom FFs exist in many versions and alterations developed by years of development, and although, in general, the accuracy of modern FFs is much better than of the old ones, not always new versions are universally better. For instance, they may overestimate the alpha [29] or beta [30] content. Thus, one should always be aware of possible bias of the method [31]. Some popular versions of FFs used to study protein systems are Amber ff99sb [32], ff14sb [33], and new ff19s [34], which is recommended to be used with more advance water model, e.g., 3-charge, 4-point rigid water model OPC [35] instead of regular three-site water model TIP3P [36]. CHARMM C22/CMAP (C27) [37, 38], C36 [39], and new C36m [40] designed with improvements for regular and disordered proteins, GROMOS

54A7 and 54B7, which improved the stability of proteins compared to 53A6 [41] and newer 54A8 [42] which fixed charge interactions [43], OPLS-AA [44], OPLS-AA-L [45], and other modifications, such as L-OPLS [46] and OPLS-AA/M [47, 48].

Additional issue is caused by peptides and proteins without stable secondary and tertiary structures, such as intrinsically disordered proteins (IDPs) [49], for which FFs often overestimate structure stability; therefore, some variants specially designed for these cases were developed [50], such as Amber ff14IDPs [51], and further improved versions ff14IDPSFF [52] and CHARM-M36IDPSFF [53], significantly improving agreement of the simulations with the experimental observables [54]. As water models can significantly change the properties of disordered proteins [55, 56], due to strong interaction of such molecules with water [57, 58], Table 1 shows short summary of popular state-of-the-art FFs with recommended water models coupled with them.

2.2 Applications of All-Atom Models

Due to computational limitations, for many years most of the applications of all-atom FFs focused on single peptide or protein systems [69]. Klimov and Thirumalai [70] were the first to apply an all-atom model to study the aggregation of three short peptides $A\beta_{16–22}$ (KLVFFAE), which stimulated a lot of works in this area. Interesting approach to overcome the problem of too short computational time to study aggregation effect in large systems was to study the addition of the monomeric chain to oligomers and fibrils, which showed the two-stage dock-and-lock mechanism of such process if oligomer is big enough [8]. Sometimes the aggregation can be studied by using even only two chains or many chains but heavily truncated, if a good description of this process can be provided [71]. A good example is studies in which possibility of the aggregation was investigated by measurement of fibril-prone structure population [72], as in the works of Viet and Li, who demonstrated that addition of Aβ40 inhibits Aβ42 aggregation [73]. Thanks to the truncation, it is possible to investigate aggregation of dimers, trimers, and bigger oligomers [74] using enhanced sampling methods, such as replica exchange molecular dynamics [75–77], which allows to overcome energy barriers and, therefore, study the conformational space more thoroughly. On the other hand, we found that in case of monomeric IDPs with the use of modern FFs, it may be enough to use conventional MD simulations, which can be speed-up by using GP-GPU calculations [78, 79], due to small energy barriers between various conformations [58]. It is especially useful because studies of monomers' beta content may be enough to predict their aggregation rates [80]; however, it is important to remember that aggregation rate alone does not provide any information about conformation and toxicity of aggregates, and some small changes in the sequence may, e.g., induce the formation of nontoxic ellipse-like aggregates

Table 1
Summary of the modern all-atom FF for studying structured proteins and IDPs. Official distributions of the FF versions are highlighted by gray background. In "Systems" column, letters S and D indicate that FF is suitable for structured or/and disordered proteins, respectively

FF	Parameters	Systems	Notes	Ref.	Recommended water model	Ref.
AMBER	ff99sb	S	Old and very popular FF	[32]	TIP3P	[36]
	a99SB-disp	S + D	Optimized a99SB-ILDN FF	[59]	TIP4P-D	[55]
	ff99SBnmr2	S + D	Improved ff99SBnmr1 FF	[60]	TIP3P for folded and TIP4P-D for IDPs	[36,55]
	ff03CMAP	S + D	Correction maps [CMAP]-optimized ff03sb FF.	[61]	TIP4P-Ew for folded and TIP4P-D for IDPs	[55,62]
	ff14sb	S	Improved ff99sb by tuning dihedral potentials	[33]	TIP3P	[36]
	ff14IDPs	D	ff14sb FF with modifications for 8 residues.	[51]	TIP3P	[36]
	ff14IDPSFF	D	ff14sb FF with modifications for 8 residues.	[52]	TIP3P	[36]
	ESFF1	S + D	Extended ff14sb FF with 71 backbone CMAP energy terms	[63]	TIP4P-D	[55]
	ff19sb	S + D	Improved backbone profiles from ff14sb.	[34]	OPC	[35]
CHARMM	C22	S	Very old and popular version of the FF	[37]	TIP3P	[36]
	C22/CMAP	S	C22 with inclusion of an energy correction map [CMAPs]	[38]	Modified TIP3P	[64]
	C36	S	Recent version of the FF for regular proteins	[39]	Modified TIP3P [ε_h= −0.046 kcal/mol]	[39]
	C36m	S + D	Optimized C36 FF with emphasis on disordered proteins	[40]	Modified TIP3P [ε_h= −0.100 kcal/mol]	[40]
	CHARMM36IDPSFF	D	C36m with modified CMAP parameters for 20 residues.	[53]	Modified TIP3P [ε_h= −0.100 kcal/mol]	[40]

(continued)

Table 1
(continued)

GROMOS	54A7	S	Popular FF version	[41]	SPC	[65]
	54A7_β	S	Optimization of beta-structures in 54A7 FF	[66]	SPC	[65]
	54A8	S	54a7 with recalibrated nonbonded interactions of charged residues	[42]	SPC	[65]
OPLS	OPLS-AA	S	All-atom version of OPLS FF	[44]		
	OPLS-AA-L	S	OPLS-AA with optimized key Fourier torsional coefficients	[45]		
	OPLSIDPSFF	S	Residue-specific variant of OPLS-AA-L FF	[67]	TIP4P-D	[55]
	L-OPLS	S	Improved treatment of long hydrocarbons [e.g. lipid bilayers]	[46]	TIP3P-MOD	[68]
	OPLS-AA/M	S + D	Improved OPLS-AA FF for proteins with additional parameters for nucleic acids	[47,48]	TIP3P	[36]

[81]. Another important note is that one should be careful when studying truncated systems, because lack of even one or two amino acid residues can significantly change their properties, such as aggregation rate, which is especially true for IDPs [82]. Influence of lipid bilayer on the amyloid peptide aggregation and peptide on bilayer stability was also investigated for monomers [83], dimers [84], and tetramers [85] including the structures manually inserted into the membrane forming beta-barrel structures [86], which were found also experimentally [87]. In case of amyloid beta, it is equally important to study aggregation of the chains as the inhibition of this process, due to the presence of different compounds, such as fullerenes [88] and their derivatives [89], curcumin [90], or small peptides [91]. Such attempts are conducted by many groups in order to provide theoretical background for fibril-related disease [10]. Computational studies of aggregates of amyloidogenic polypeptides such as Aβ, α-synuclein, islet amyloid polypeptide, tau protein, and prion protein have been recently reviewed by Ilie and Caflisch [92].

3 Coarse-Grained Models

In general, idea of coarse-graining is based on the assumption that reduction of the interacting centers decreases the computational time required for every MC or MD step and that conformational space can be searched more thoroughly due to smoother energy landscape (Fig. 3) and better sampling. Simplification of the system representation always bears a risk that some important details will be missing, negatively impacting accuracy of the method [93, 94]; therefore, users should be even more careful to check if a given approach provides satisfactory results for the investigated phenomenon [95, 96]. On the more positive side, coarse-grained FF can provide much wider view than all-atom methods, due to ability to study system or phenomenon much more extensively, using higher number of longer trajectories, providing better statistics and average properties than single-trajectory studies and discover secondary pathways of some processes [97]. All types of coarse-grained FFs, including structure-based, knowledge-based, and dynamics-based model, are currently very intensively developed to allow reliable simulations of macromolecular complexes [98]. Additionally, there are approaches to develop and use multiscale coarse-grained simulations to study biological systems [99, 100], or to include polarization [101] and reactivity [102]; there are not yet advanced enough to use for complex biomacromolecular systems.

3.1 Typical FFs Used for Studies of Systems Involving Peptides or Proteins

Although there are many in-house coarse-grained FFs dedicated for studies of very limited number of systems, or even single cases [103, 104], there are also general-purpose coarse-grained FFs, such as AWSEM [105], CABS [106], MARTINI [107, 108],

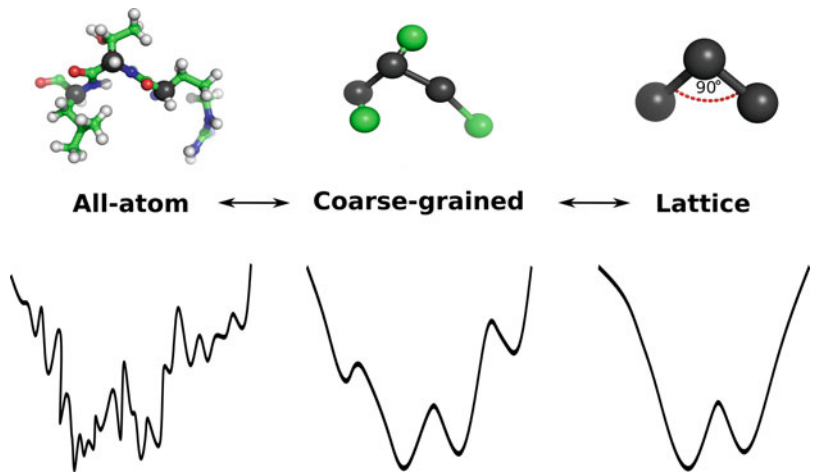

Fig. 3 Schematic representation of the all-atom, coarse-grained, and lattice representations and respective energy landscapes

OPEP [109, 110], PaLaCe [111], PRIMO [112], SIRAH [113, 114], and UNRES [115–117]. Contrary to the all-atom FFs, coarse-grained ones differ significantly not only in parameters of interacting centers, but also in system representation (level of reduction) and energy functions [93, 118]. Although such universal FFs allows in principle to study a plethora of phenomena, such as protein folding, conformational changes, and aggregation, due to complexity of these processes, performance of every method should be verified before application. One good example is the MARTINI FF, which was found to cause excessive, irreversible, and non-selective aggregation of membrane proteins [119], which is one of the problems assigned to be fixed in the next version of the FF [120]. Another issue comes from the unstructured character of IDPs, which are poorly described by most of the FFs, mostly due to overestimation of secondary structure stability. In some cases, it can be simply fixed by tuning energy potential terms responsible for secondary structure, like in ASWEN-IDP [121] or increasing strength of protein–water interactions [122]; however, sometimes design of the completely new method instead of modifying existing one is more convenient, like in case of FRAGFOLD-IDP [123], being redesigned CABSFlex [124]. One should have in mind that although design of IDP-specific version of the method should improve performance for these proteins, it may corrupt results for regular systems. Another problem may come from the fact that majority of coarse-grained FFs use knowledge-based potentials to describe studied systems. Their usage to study aggregation of IDPs, such as Aβ42, may be problematic, due to the fact that they are strongly biased by the structures deposited in the Protein Data Bank [125], used for parametrization, which are available only for fibrils, not for monomeric or oligomeric forms in water.

3.2 Applications of General-Purpose Coarse-Grained FFs

Despite the limitations, at some point every popular coarse-grained FF was successfully used to study aggregation or oligomerization-related effects. It is unavoidable, as it is predicted that more than 80% of proteins stay not alone in the cell, but in complexes [126]. A few examples are presented below. The AWSEM Amylometer is a useful and powerful tool for prediction of amyloidogenic segments from the sequence providing additional information of thermodynamic and kinetic roles of these segments in folding and aggregation based on AWSEM FF [127]. Very recently, the same FF was used to study nucleation of two fibrils derived from patients with Pick's and Alzheimer's diseases showing importance of oligomeric structure on the fibrilization: oligomers with parallel in-register β-strands lead to fibril formation, while not ordered β-strand stacking lead to amorphous structures [128]. Even though in the

MARTINI model, secondary structure is fixed during simulation, there are still some attempts, in which it can be successfully used for structural studies of aggregation dynamics of self-assembling systems, such as self-assembling peptides [129], dipeptides [130] and other short peptides [131], and even effect of lipid bilayer on Aβ peptide [132]. Newer FFs, like PRIMO and PaLaCe, were not extensively used yet, but even for them they are examples of association studies [133].

Various coarse-grained FFs are used to study also aggregation process of other molecules, such as α-synuclein, for which it was found that formation of β-hairpin in region 38–53 is necessary for the aggregation [134] and that non-amyloid-β component (NAC) mutations can disturb aggregation [135]. Influence of some molecules, like trehalose, which promote alternate aggregation pathway leading to the formation of amorphous aggregates was also studied as a possible way to treat Parkinson disease [136]. Another molecule, which is commonly studied for aggregations effect, is tau protein, for which nucleation kinetics of hexapeptide fragments involved in fibril formation was extensively studied by a coarse-grained FF [137], as well as effect of the temperature on fibril formation [138].

3.3 OPEP Coarse-Grained FF

The most extensively used coarse-grained FF for studies of peptide and protein aggregation is OPEP (Optimized Potential for Efficient Protein Structure Prediction), developed by the group of Philippe Derreumaux for more than 20 years [109]. In OPEP, protein chain representation is reduced this way that the backbone consists of all atoms (N, Cα, C, O, and H), while side chain is simplified to coarse-grained form (one bead, except for proline, which is described by all heavy atoms) to find good compromise between accuracy and speed-up [139]. Authors not only carefully designed the FF and model, but extensively tested it for protein folding capabilities [140], pH dependence [141], and investigated influence of simulation temperature [142] and thermostat on the obtained results [143].

Using ART-OPEP simulations, it was demonstrated that the formation of oligomeric metastable structures is an important step in fibrilization process and provided possible explanation of dependency of β-sheet formation on pH conditions [144]. Later, using OPEP and all-atom FF, it was presented that the formation of stable β-barrel structures of NHVTLSQ oligomers [145] may be an important early aggregation step in fibril formation process [146]. Very recently, the same group demonstrated using all-atom methods that similar structures may be obtained by truncated $A\beta_{11-40}$ in dipalmitoylphosphatidylcholine membrane models [147]. In other recent studies, OPEP was used to study 1000

chains of very truncated $A\beta_{16–22}$ to show prefibril elongation mechanism, including pore and branch formation during aggregation process [148]. Thanks to the addition of the hydrodynamical effects to the OPEP FF, it can better capture kinetics of aggregation and association processes, speeding-up the collapse of molecules by about 40% [149].

3.4 UNRES Coarse-Grained FF

UNRES (UNited RESidue) is a coarse-grained physics-based FF, in which polypeptide chain representation is reduced to two interaction centers: peptide and side chain. It has been developed for more than 20 years by Liwo, Scheraga, and coworkers to allow realistic studies of peptides and proteins. It allows to study ab initio folding processes of many single-chain [95, 150, 151] and multi-chain proteins [152] including their aggregation for two [153], four [154, 155], and more chains with a good accuracy, if the satisfactory simulation time can be reached. UNRES can work purely as an ab initio method, without any information from databases, or to utilize in simulations some information, like predicted contacts between residues [156], SAXS data [157] or domain [158], and protein fragment [159] structures.

In the past, UNRES was used to study the growth mechanism of Aβ fibrils by adding monomer to the existing fibril template without any additional bias, which allowed to confirm the dock-lock mechanism with two distinct locking stages and importance of hydrophobic contacts between chains [160]. These studies were recently extended to determine most probable pathways of fibril elongation and residues necessary for the process to occur [161]. Also the importance of α-to-β transition of 17–21 residue fragment was found by the molecular dynamics simulation in UNRES FF to allow propagation along the 28-residue amino-terminal fragment of Aβ chains [162]. It was demonstrated that in the presence of extended 16–21 residue fragment of Aβ (such as in fibrils, but not in monomers), Aβ can bind to repeat domain of tau forming Aβ40 fibril–tau aggregates [163]. In the most recent studies, we showed using multi-scale simulations that tetrameric structures of Aβ significantly differ from Aβ fibrils [155] and that Aβ–water interactions are key for stabilization of monomers [58] and small oligomers. We also showed that the formation of the tetramer is mostly due to interaction between two dimers, rather than trimer and monomer (Fig. 4) what was suggested also by other studies using OPLS/AA FF [164].

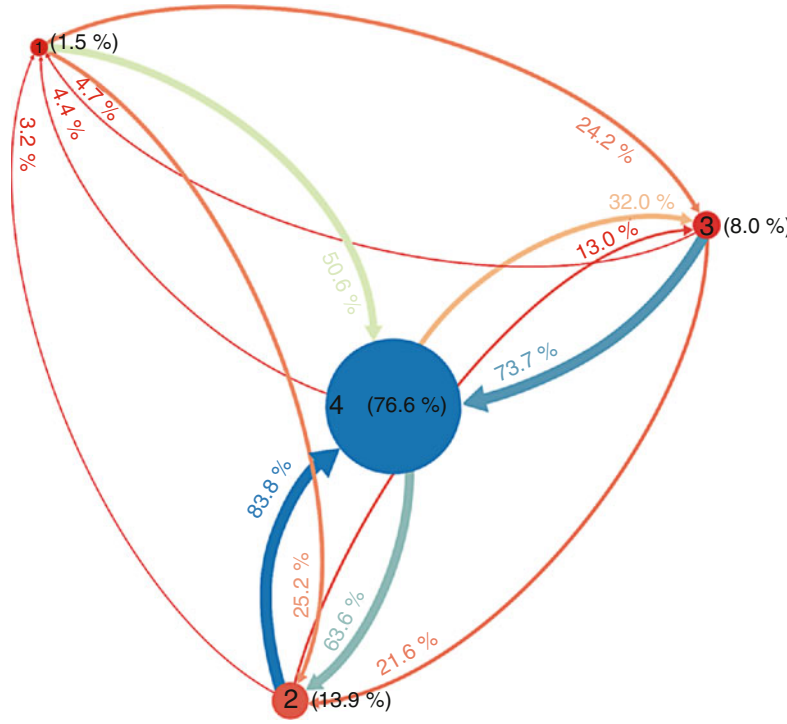

Fig. 4 Transition network from UNRES REMD simulation showing oligomer size (label on each node) and transitions between different forms (arrows) [155]

4 Other Off-Lattice Coarse-Grained FFs

In the following paragraphs, some off-lattice coarse-grained models designed and applied for the study of peptide aggregation are briefly described. Since there are many models of these types, for convenience we call them after the name of the authors who have developed them. Representation of amino acids in most of the models described below is more simplified than in general-purpose coarse-grained FFs.

4.1 The Vacha–Frenkel Model

Vacha and Frenkel constructed a generic CG model, in which the peptides had patchy sphero-cylinder's (PSC) shape with a stripe on its side representing their binding ability. Using Monte Carlo simulations, the authors proved that this model can successfully predict the existence of oligomeric states capturing a two-filament amyloid-like structure [165]. Then, in the two-state modified model, specifically designed to describe Aβ peptides, the patchy particles can switch between α- or β-states corresponding to the soluble peptide or extended peptide conformation in Aβ-amyloid structure, respectively. By performing 2μs of Dynamic Monte Carlo (DMC) simulation for a system of 600 PSCs, the authors were able to observe

fibrillar species with a morphology similar to experimental observations. The kinetics of patchy self-assembly is consistent with Oosawa's theory and the critical nucleation size was estimated to be about 3.8 chains [166]. Based on the PSC model, properties of the fibrillar nucleation-dependence kinetics were further studied [167–169], and the effect of various surfaces on the rate of amyloid formation was systematically investigated [170].

4.2 The Barz–Urbanc Model

Barz and Urbanc defined the unit of their minimal self-assembly model as a tetrahedron of two attractive (hydrophobic) and two repulsive (hydrophilic) beads located at its vertices [171]. The model employed a discrete MD algorithm combined with periodic boundary condition and an implicit solvent. By modulating the values of the hydropathic parameter η, the ratio between repulsive and attractive interaction, the authors obtained various morphologies of aggregates such as quasi-spherical oligomers, curved tubules, curvilinear protofibrils, and multi-domain aggregates. The mechanism of monomer addition, assembly fusion, and breakdown has also been reported [171].

4.3 The Hoang–Trovato–Seno–Banavar–Maritan Model

Auer et al. extended Hoang-Trovato-Seno-Banavar-Maritan tube model [172], in which each residue is simplified to Cα atom, represented as a flexible tube, in order to study the nucleation and growth mechanism of peptide fibrillation [173] and to shed light on the kinetics of conversion from disordered oligomer species into protofilaments [174]. Hoang et al. applied the model to study the sequence dependence of the aggregation process, stating that the fibril template created by highly fibril-prone sequences can assist the formation of poorly amyloidogenic sequences into a fibril-like structure [175].

4.4 The Mioduszewski–Cieplak Model

Cieplak and Mioduszewski developed one-bead-per-residue Cα model to investigate intrinsic disorder proteins using unique design in which contacts between beads can form and disappear during MD simulation [176]. Using their model, the authors successfully constructed the polyglutamine and polyalanine phase diagrams which not only confirmed the existence of liquid–gas coexistence curve at room temperature but also revealed a novel amyloid-glass phase corresponding to the fibril-liked structures of the proteins at low temperatures [177]. Recently, the model was updated with the introduction of nonradial multibody pseudo-improper-dihedral potentials which allowed to more accurately capture protein and protein assembly properties during MD simulations [178].

4.5 The Ilie–den Otter–Briels Model

Ilie and coworkers developed a highly CG polymorph patchy particle model [179] to study α-synuclein and its self-assembly. In their model, the protein is treated as a particle, and a changeable internal state was assigned to characterize the structural adaptability of this intrinsically disordered protein.

The disordered state and β-sheets are described as a solid sphero-cylinder with a long attractive stripe and soft spheres, respectively. The probability of shifting between the two states was set to favor the ordered state for bound particles. The authors matched the particle parameters to the experimental data of α-synuclein and performed Brownian dynamics simulations. They found that the kinetics of fibril formation confronted to either the nucleation and growth mechanism or a two-step mechanism. Furthermore, the preformed fibrils promoted the conversion of oligomers to fibrils. The authors also introduced a higher resolution version of α-synuclein as a mixture connecting polymorph particles and examined the kinetics of peptides incorporation at the fibril end [180].

4.6 The Pellarin–Caflish Model

Pellarin and Caflish developed a two-state CG phenomenological model of a simple amphipathic peptide consisting of ten beads, of which six beads described the peptide side chain and the remaining four served as its backbone [181]. The peptide can rotate around its internal dihedral, which is a unique freedom degree of the system, to switch between amyloid-competent (β) and amyloid-protected states (π), and the energy barrier between the two states modulates the degree of amyloidogenicity of the peptide. For highly amyloid-prone chains (HAPs), aggregation events occurred even at concentrations lower than the critical concentration of micelle (CMC), and the fibril mass was accumulated directly through a single pathway of a small nucleus without micelles, as well as intermediate protofibrils with the growth rate strongly dependent on the peptide concentration. Poorly amyloid-prone (PAPs) proteins nucleated through multiple pathways with a large nucleus at concentrations above CMC and fibril formation proceeded slowly through different metastable intermediates. It was found that the concentration of molecules has little impact on the fibril growth rate [181, 182]. Their simulation results also indicated that HAPs favorably formed the fibril morphology with the highest stability, while for PAPs, the formation of the fibril shape was regulated by kinetics [183]. Additionally, self-assembly of PAPs was accelerated by the crowding effect, retarded by membranes as well as surfactants, but does not play a clear role in membrane leakage. Whereas, the process of fibril formation of HAPs promoted membrane leakage is lightly enhanced by membranes, but is not sensitive to crowders and marginally influenced by surfactants [184–186].

4.7 The Bellesia–Shea Model

Each amino acid residue in the Bellesia–Shea model [187] is represented by three beads, two beads for the backbone and one for the sidechain. The authors introduced four different types of side chains: hydrophobic, polar, positively and negatively charged, and end group capped at both termini of the peptide to prevent edge-to-edge aggregation. The dihedral potential of the backbone was used to alter the β-sheet propensity of peptides. The model shared a

similar self-assembly kinetics with the Pellarin–Caflisch CG model [188], for HAPs the aggregation pathway included a small ordered β-strand forming nucleus, which subsequently acted as a template for fibril growth, while for PAPs, initially formed amorphous clusters gradually transforming into ordered structures. Bellesia–Shea model can capture diverse structures such as disordered oligomers, beta barrels, and multilayer fibrils. Simulations in the presence of absorbing solid foreign surfaces and lipid bilayers membranes showed that both environments promote the formation of the β-sheet motif near the surfaces [189].

5 On-Lattice Models for the Study of Protein Aggregation

This part discusses the most simplified on-lattice coarse-grained models used to study protein aggregation. Such models are usually designed to solve a specific problem and focus on general physical principles, rather than on biology. In particular, we pay more attention to the lattice model, originally constructed by Li, Klimov, and Thirumalai [190], and then developed and extended by Li and Co [191–195] to various systems.

5.1 The Irback–Jónsson–Linnemann–Linse–Wallin model

Irback et al. designed a model [196], in which the peptides are represented by unit-length sticks located on lattice sites. Each peptide consists of three vectors characterizing the backbone, hydrogen bond, and side chain orientation (Fig. 5a). The movement of sticks is enabled through a MC algorithm. MC simulations

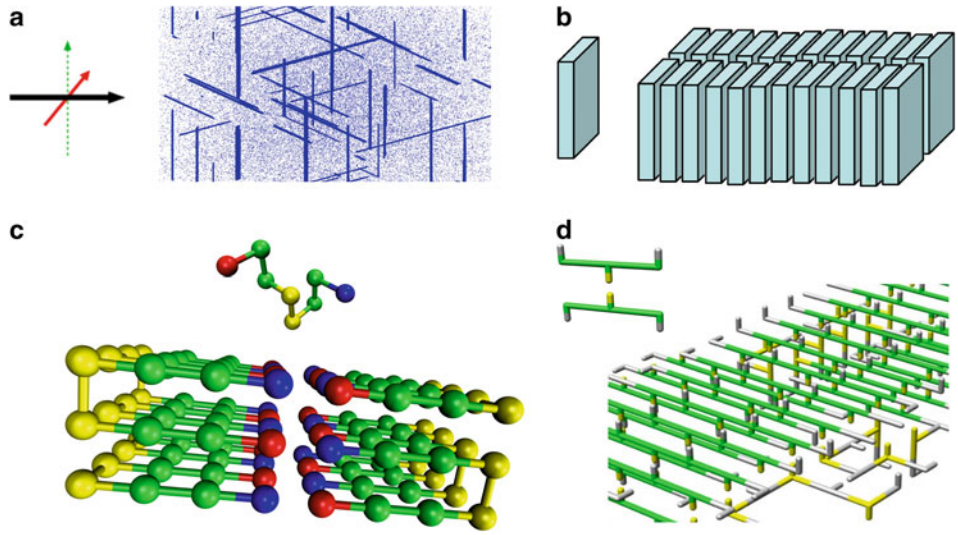

Fig. 5 Monomers and fibril-like structures in several lattice models. (**a**) Stick model [196], (**b**) cuboid model [197], (**c**) one-bead lattice model, (**d**) multi-bead lattice model [198] (the small part represents a fragment of peptide)

of more than 105 monomers allowed to capture the sigmoid kinetics of fibrillar growth. In addition, the interplay between length and width during the fibril nucleation indicated that the longitudinal growth of fibril-like structures occurs only after their width reaches a threshold value [196].

5.2 The Zhang–Muthukumar Model

To study the nucleation and elongation of amyloid fibrils, Zhang and Muthukumar developed a lattice model, in which monomers are represented by cuboid unit cells in a cuboidal simulation box (Fig. 5b) [197]. A unit cell can reflect an extended peptide, a folded peptide, and a pair of peptides, and its random movements are allowed by MC random walks. The simulation result showed that the aggregation of monomers followed nucleation-dependent behavior, in which the lag phase and elongation stage follow the Ostwald ripening mechanism [197].

5.3 The Abeln–Vendruscolo–Dobson–Frenkel Model

Abeln et al. have developed a multi-bead lattice model allowing to study the interplay between fibrillization and folding processes (Fig. 5d) [198, 199]. In this model, each residue comprises one bead located at a lattice site and a vector representing the directionality of the side chain. Vacant lattice sites describe the surrounding solvent and possibly interact with both the backbone and side chains. The classical MC simulation showed that a predefined folding structure can be achieved by careful design of the peptide sequence. The authors also obtained the β-strand motif in both folded structure and fibrillar species. In addition, Tran and coworkers implemented the OPEP FF to the Abeln–Vendruscolo–Dobson–Frenkel model and performed simulations of aggregation of truncated Aβ peptides to estimate their critical nucleus size [200].

5.4 The Li–Klimov–Straub–Thirumalai Model

Inspiring by the oligomerization of the $A\beta_{16–22}$ fragments, Li et al. developed a simple on-lattice model, where a polypeptide chain has eight beads +HHPPHH−. Here + and − stand for positively and negatively charged beads, respectively, while P and H refer to polar and hydrophobic residues (Fig. 5c) [190]. The interactions between the pairs of residues were chosen so that they roughly mimic the real properties. In Monte Carlo simulations, the peptides changed their configuration through random local and global moves in combination with the classical Metropolis algorithm. The fibrillar structure (Fig. 5c) corresponds to the lowest energy. The model can describe the typical sigmoidal dependence of the fibril mass on the simulation time involving the lag, growth, and saturation phases (Fig. 2). Furthermore, three popular types of kinetics have been observed at various stages in the fibril formation process, including nucleation and growth, templated assembly, as well as nucleated conformational conversion [190].

The Li–Klimov–Straub–Thirumalai model has been used to systematically study the factors that govern the kinetics of protein aggregation. It was found [191] that the stronger attractive electrostatic and hydrophobic interactions between the polypeptide chains, the faster fibril formation, which is consistent with the experiment [201, 202]. Interestingly, the fibril formation time τ_{fib} exponentially depends on the population of the fibril-prone monomeric state N* (Fig. 6a), P_{N}*: $\tau_{\text{fib}} = \tau_{\text{fib}}^{0} \exp\left(-cP_{\text{N}^*}^{\max}\right)$, where τ_{fib}^{0} and c are fitting constants. Our studies using all-atom models supported this conclusion [80].

Similar to the experimental [203] and simulation results obtained using the Pellarin–Caflish models [181], for HAPs, we observed a direct association of peptides to form rich β-strand clusters during an early stage of aggregation. The fibril growth phase appears only after the formation of a critical nucleus, from which monomers favor to incorporate into the template. Based on this argument, we designed various systems, including a rich β preformed template and one separate peptide (Fig. 6b) and measured adding time τ_{add} (the time required for a peptide to assemble into its template). Simulations showed that τ_{add} increased until the size of the preformed template reaches the critical nucleus size (N_{c}), above which τ_{add} becomes independent of the template size. The obtained N_{c} value agreed well with the critical nucleus size estimated by the

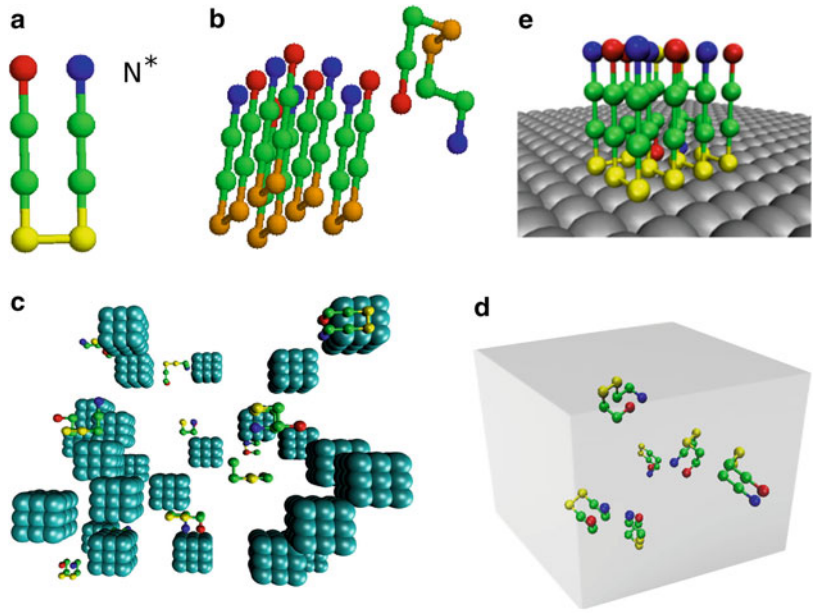

Fig. 6 The factors governing the self-assembly rate uncovered by using Li–Klimov–Straub–Thirumalai lattice model: (**a**) Fibril-prone state N*, (**b**) preformed template and adding monomer, (**c**) snapshot of polypeptide chains surrounded by cubic crowders, (**d**) six peptides in a confined box, (**e**) fibril structure of six chains on a hydrophilic smooth surface

free energy scaling method [193, 204]. In addition, using all-atom simulations, we proved that the pathways of fibril formation from the immobilized template (monomers in the template were kept fixed) must cross more intermediate states than paths starting from the fluctuating template. Consequently, the fluctuating template assisted the fibril formation better than the immobile template. As a result, the template fluctuation can be considered as a factor controlling the aggregation process, and the slow formation of mature fibril structures during the saturation phase is probably due to the rigidity of their preformed template [194].

To study the impact of the environment on the fibril growth kinetics, cube crowders were added to the Li–Klimov–Straub–Thirumalai model (Fig. 5c). They can make self-avoiding random walks and do not interact with each other, nor with peptides. Having carried out simulations with various concentrations and sizes of crowders, we captured the excluded volume effect of crowding particles [205, 206]. For a given crowder size, the presence of the milieu restricted the space for peptides resulting in accelerated self-assembly of the chains. This observation well matched with the previous theoretical [207] and experimental works [185, 208]. However, when the size of crowders was sufficient small, they hindered the aggregation process, and this dual effect is consistent with the experiment of Cabaleiro-Lago et al. [209]. Besides, the study of protein fibrils in a confinement space was performed by switching periodic boundary conditions and changing the size of the simulation box (Fig. 6d). The compromise between energetic terms and entropy resulted in a U-shape dependence of τ_{fib} on the size of the confining box [192].

Combing the Li–Klimov–Straub–Thirumalai model with all-atom models, we were able to show that the higher the mechanical stability of the fibril state, the faster the fibril formation [195] which is partly consistent with the experiment. However, this hypothesis requires further computational and theoretical support.

Finally, we also used our simplified model as a guide tool to develop a phenomenological theory to explain the mechanism of heat-induced degradation of fibrils and to explore the effect of different surfaces on peptide assembly [210]. We have shown that the time dependence of the fibril content, which can be measured by the ThT fluorescence assay, obeys a bi-exponential function. However, the number of unbounded chains, which can be probed by tryptophan fluorescence, follows the logistic kinetics.

6 Conclusions

In conclusion, we highlight future directions in the development of computational models to study protein folding and aggregation.

A good example of use of the all-atom FF to study enormous systems was done by Sugita, Feig and coauthors, who studied bacterial cytoplasm with more than 100 million atoms in a nanosecond timescale [211]. These simulations showed possible problems with the FF, which were not possible to be identified in simulations of smaller systems and presented view of proteins and other biomacromolecules in crowding environment, whose behavior can be significantly different than in bulk water [211] mostly due to confined space and presence of nonspecific interactions between molecules, which can affect protein stability [212], folding, and aggregation [213]. Although limited timescale of the simulations did not allow study protein aggregation explicitly, obtained results strongly suggest that this phenomenon should be studied including other molecules, which are competing in interactions, destabilizing the structure and promoting association [214]. Due to the constant improvement and development of both computational resources and methods [215, 216], in near future such large-scale studies should become more affordable and may even allow to use polarizable FFs [217, 218] to better capture effects related to charge distribution. It is well known that the presence of metal ions can change not only the aggregation rate but the morphology of the aggregate [219]. For example, at high concentrations of Cu^{2+}, the aggregate of Aβ peptides becomes amorphous. The development of FFs that adequately describe free transition metal ions and their interaction with fibril-prone proteins remains a challenge. Finally, machine learning is emerging as a useful tool for constructing coarse-grained FFs from large ab initio databases [220], and important advances in this direction can be expected.

Acknowledgments

We appreciate collaboration with Hoang Linh Nguyen. This research has been supported by Narodowe Centrum Nauki in Poland (Grant 2019/35/B/ST4/02086), the Department of Science and Technology at Ho Chi Minh city (Grant 07/2019/HĐ-KHCNTT), the Vietnam Ministry Education and Training (Project B2019.SPD.03), Vietnam.

References

1. Chiti F, Dobson CM (2006) Protein misfolding, functional amyloid, and human disease. Annu Rev Biochem 75:333–366
2. Hardy JA, Higgins GA (1992) Alzheimer's disease: the amyloid cascade hypothesis. Science (80-) 256:184–185
3. Spillantini MG, Crowther RA, Jakes R et al (1998) α-Synuclein in filamentous inclusions of Lewy bodies from Parkinson's disease and dementia with Lewy bodies. Proc Natl Acad Sci U S A 95:6469–6473
4. Bernstein SL, Dupuis NF, Lazo ND et al (2009) Amyloid-β protein oligomerization and the importance of tetramers and dodecamers in the aetiology of Alzheimer's disease. Nat Chem 1:326–331

5. Jarrett JT, Lansbury PT (1993) Seeding "one-dimensional crystallization" of amyloid: a pathogenic mechanism in Alzheimer's disease and scrapie? Cell 73:1055–1058
6. Harper JD, Lansbury PT (1997) Models of amyloid seeding in Alzheimer's disease and scrapie: mechanistic truths and physiological consequences of the time-dependent solubility of amyloid proteins. Annu Rev Biochem 66:385–407
7. Hofrichter J, Ross PD, Eaton WA (1974) Kinetics and mechanism of deoxyhemoglobin S gelation: a new approach to understanding sickle cell disease. Proc Natl Acad Sci U S A 71:4864–4868
8. Nguyen PH, Li MS, Stock G et al (2007) Monomer adds to preformed structured oligomers of Aβ-peptides by a two-stage dock-lock mechanism. Proc Natl Acad Sci U S A 104:111–116
9. Cohen SIA, Linse S, Luheshi LM et al (2013) Proliferation of amyloid-β42 aggregates occurs through a secondary nucleation mechanism. Proc Natl Acad Sci 110:9758–9763
10. Nasica-Labouze J, Nguyen PH, Sterpone F et al (2015) Amyloid β protein and Alzheimer's disease: when computer simulations complement experimental studies. Chem Rev 115:3518–3563
11. Wu C, Shea JE (2011) Coarse-grained models for protein aggregation. Curr Opin Struct Biol 21:209
12. Morriss-Andrews A, Shea J-E (2015) Computational studies of protein aggregation: methods and applications. Annu Rev Phys Chem 66:643–666
13. Chong S-H, Chatterjee P, Ham S (2017) Computer simulations of intrinsically disordered proteins. Annu Rev Phys Chem 68:117–134
14. Anfinsen CB (1973) Principles that govern the folding of protein chains. Science (80-) 181:223–230
15. Levinthal C (1969) How to fold graciously. In: Debrunner P, Tsibris J, Munck E (eds) Mossbauer spectroscopy in biological systems: Proceedings of a Meeting Held at Allerton House, Monticello, Illinois. University of Illinois Press, Champaign, IL, pp 22–24
16. Levinthal C (1968) Are there pathways for protein folding? J Chim Phys 65:44–45
17. Hartl FU, Hayer-Hartl M (2009) Converging concepts of protein folding in vitro and in vivo. Nat Struct Mol Biol 16:574–581
18. Frozza RL, Lourenco MV, Felice FG (2018) Challenges for Alzheimer's disease therapy: insights from novel mechanisms beyond memory defects. Front Neurosci 12:37
19. Viña J, Sanz-Ros J (2018) Alzheimer's disease: only prevention makes sense. Eur J Clin Investig 48:e13005
20. Weiner PK, Kollman PA (1981) AMBER: assisted model building with energy refinement. A general program for modeling molecules and their interactions. J Comput Chem 2:287–303
21. Brooks BR, Bruccoleri RE, Olafson BD (1983) CHARMM: a program for macromolecular energy, minimization, and dynamics calculations. J Comput Chem 4:187–217
22. Hermans J, Berendsen HJC, Gunsteren WFV et al (1984) A consistent empirical potential for water-protein interactions. Biopolymers 23:1513–1518
23. Jorgensen WL, Tirado-Rives J (1988) The OPLS [optimized potentials for liquid simulations] potential functions for proteins, energy minimizations for crystals of cyclic peptides and crambin. J Am Chem Soc 110:1657–1666
24. Gunsteren WFV, Berendsen HJC (1977) Algorithms for macromolecular dynamics and constraintdynamics. Mol Phys 34:1311–1327
25. Andersen HC (1983) Rattle: a "velocity" version of the shake algorithm for molecular dynamics calculations. J Comput Phys 52:24–34
26. Miyamoto S, Kollman PA (1992) Settle: an analytical version of the SHAKE and RATTLE algorithm for rigid water models. J Comput Chem 13:952–962
27. González MA (2011) Force fields and molecular dynamics simulations. Collect SFN 12:169–200
28. Lopes PEM, Guvench O, MacKerell AD (2015) Current status of protein force fields for molecular dynamics simulations. Methods Mol Biol (Clifton, NJ) 1215:47–71
29. Garcia AE, Sanbonmatsu KY (2002) α-helical stabilization by side chain shielding of backbone hydrogen bonds. Proc Natl Acad Sci U S A 99:2782–2787
30. Ono S, Nakajima N, Higo J et al (2000) Peptide free-energy profile is strongly dependent on the force field: comparison of C96 and AMBER95. J Comput Chem 21:748–762
31. Freddolino PL, Park S, Roux B et al (2009) Force field bias in protein folding simulations. Biophys J 96:3772–3780
32. Hornak V, Abel R, Okur A et al (2006) Comparison of multiple Amber force fields and

development of improved protein backbone parameters. Proteins Struct Funct Bioinf 65:712–725

33. Maier JA, Martinez C, Kasavajhala K et al (2015) ff14SB: improving the accuracy of protein side chain and backbone parameters from ff99SB. J Chem Theory Comput 11:3696–3713
34. Tian C, Kasavajhala K, Belfon KAA et al (2020) Ff19SB: amino-acid-specific protein backbone parameters trained against quantum mechanics energy surfaces in solution. J Chem Theory Comput 16:528–552
35. Izadi S, Anandakrishnan R, Onufriev AV (2014) Building water models: a different approach. J Phys Chem Lett 5:3863–3871
36. Jorgensen WL, Chandrasekhar J, Madura JD et al (1983) Comparison of simple potential functions for simulating liquid water. J Chem Phys 79:926–935
37. MacKerell AD, Bashford D, Bellott M et al (1998) All-atom empirical potential for molecular modeling and dynamics studies of proteins. J Phys Chem B 102:3586–3616
38. Mackerell AD, Feig M, Brooks CL (2004) Extending the treatment of backbone energetics in protein force fields: limitations of gas-phase quantum mechanics in reproducing protein conformational distributions in molecular dynamics simulation. J Comput Chem 25:1400–1415
39. Huang J, MacKerell AD (2013) CHARMM36 all-atom additive protein force field: validation based on comparison to NMR data. J Comput Chem 34:2135–2145
40. Huang J, Rauscher S, Nawrocki G et al (2017) CHARMM36m: an improved force field for folded and intrinsically disordered proteins. Nat Methods 14:71–73
41. Schmid N, Eichenberger AP, Choutko A et al (2011) Definition and testing of the GROMOS force-field versions 54A7 and 54B7. Eur Biophys J 40:843–856
42. Reif MM, Hünenberger PH, Oostenbrink C (2012) New interaction parameters for charged amino acid side chains in the GROMOS force field. J Chem Theory Comput 8:3705–3723
43. Reif MM, Winger M, Oostenbrink C (2013) Testing of the GROMOS force-field parameter set 54A8: structural properties of electrolyte solutions, lipid bilayers, and proteins. J Chem Theory Comput 9:1247–1264
44. Jorgensen WL, Maxwell DS, Tirado-Rives J (1996) Development and testing of the OPLS all-atom force field on conformational energetics and properties of organic liquids. J Am Chem Soc 118:11225–11236
45. Kaminski GA, Friesner RA, Tirado-Rives J et al (2001) Evaluation and reparametrization of the OPLS-AA force field for proteins via comparison with accurate quantum chemical calculations on peptides. J Phys Chem B 105:6474–6487
46. Siu SWI, Pluhackova K, Böckmann RA (2012) Optimization of the OPLS-AA force field for long hydrocarbons. J Chem Theory Comput 8:1459–1470
47. Robertson MJ, Tirado-Rives J, Jorgensen WL (2015) Improved peptide and protein torsional energetics with the OPLS-AA force field. J Chem Theory Comput 11:3499–3509
48. Robertson MJ, Tirado-Rives J, Jorgensen WL (2016) Performance of protein-ligand force fields for the flavodoxin-flavin mononucleotide system. J Phys Chem Lett 7:3032–3036
49. Wright PE, Dyson HJ (1999) Intrinsically unstructured proteins: re-assessing the protein structure-function paradigm. J Mol Biol 293:321–331
50. Huang J, MacKerell AD (2018) Force field development and simulations of intrinsically disordered proteins. Curr Opin Struct Biol 48:40–48
51. Song D, Wang W, Ye W et al (2017) ff14IDPs force field improving the conformation sampling of intrinsically disordered proteins. Chem Biol Drug Des 89:5
52. Song D, Luo R, Chen H-F (2017) The IDP-specific force field ff14IDPSFF improves the conformer sampling of intrinsically disordered proteins. J Chem Inf Model 57:1166–1178
53. Liu H, Song D, Lu H et al (2018) Intrinsically disordered protein-specific force field CHARMM36IDPSFF. Chem Biol Drug Des 92:1722–1735
54. Liu H, Song D, Zhang Y et al (2019) Extensive tests and evaluation of the CHARMM36IDPSFF force field for intrinsically disordered proteins and folded proteins. Phys Chem Chem Phys 21:21918–21931
55. Piana S, Donchev AG, Robustelli P et al (2015) Water dispersion interactions strongly influence simulated structural properties of disordered protein states. J Phys Chem B 119:5113–5123
56. Best RB, Zheng W, Mittal J (2014) Balanced protein-water interactions improve properties of disordered proteins and non-specific protein association. J Chem Theory Comput 10:5113–5124

57. Gallat FX, Laganowsky A, Wood K et al (2012) Dynamical coupling of intrinsically disordered proteins and their hydration water: comparison with folded soluble and membrane proteins. Biophys J 103:129–136
58. Krupa P, Quoc Huy PD, Li MS (2019) Properties of monomeric Aβ42 probed by different sampling methods and force fields: role of energy components. J Chem Phys 151:055101
59. Robustelli P, Piana S, Shaw DE (2018) Developing a molecular dynamics force field for both folded and disordered protein states. Proc Natl Acad Sci U S A 115:E4758–E4766
60. Yu L, Li DW, Brüschweiler R (2020) Balanced amino-acid-specific molecular dynamics force field for the realistic simulation of both folded and disordered proteins. J Chem Theory Comput 16:1311–1318
61. Zhang Y, Liu H, Yang S et al (2019) Well-balanced force field ff03 CMAP for folded and disordered proteins. J Chem Theory Comput 15:6769–6780
62. Horn HW, Swope WC, Pitera JW et al (2004) Development of an improved four-site water model for biomolecular simulations: TIP4P-Ew. J Chem Phys 120:9665–9678
63. Song D, Liu H, Luo R et al (2020) Environment-specific force field for intrinsically disordered and ordered proteins. J Chem Inf Model 60:2257
64. MacKerell AD Jr, Brooks B, Brooks CL III et al (1998) CHARMM: the energy function and its parametrization with an overview of the program. Encyclop Computat Chem 1:271–277
65. Berendsen HJC, Postma JPM, Gunsteren WFV et al (1981) Interaction models for water in relation to protein hydration. In: Pullman B (ed) Intermolecular forces. Springer, Dordrecht, pp 331–342
66. Lin Z, Gunsteren WFV (2013) Refinement of the application of the GROMOS 54A7 force field to β-peptides. J Comput Chem 34:2796–2805
67. Yang S, Liu H, Zhang Y et al (2019) Residue-specific force field improving the sample of intrinsically disordered proteins and folded proteins. J Chem Inf Model 59:4793–4805
68. Sun Y, Kollman PA (1995) Hydrophobic solvation of methane and nonbond parameters of the TIP3P water model. J Comput Chem 16:1164–1169
69. Scheraga HA (1983) Recent progress in the theoretical treatment of protein folding. Biopolymers 22:1–14
70. Klimov DK, Thirumalai D (2003) Dissecting the assembly of Aβ16-22 amyloid peptides into antiparallel β sheets. Structure 11:295–307
71. Nguyen PH, Li MS, Derreumaux P (2014) Amyloid oligomer structure characterization from simulations: a general method. J Chem Phys 140:094105
72. Nam HB, Kouza M, Zung H et al (2010) Relationship between population of the fibril-prone conformation in the monomeric state and oligomer formation times of peptides: insights from all-atom simulations. J Chem Phys 132:165104
73. Viet MH, Li MS (2012) Amyloid peptide Aβ 40 inhibits aggregation of Aβ 42: evidence from molecular dynamics simulations. J Chem Phys 136:245105
74. Nguyen PH, Li MS, Derreumaux P (2011) Effects of all-atom force fields on amyloid oligomerization: replica exchange molecular dynamics simulations of the Aβ16–22 dimer and trimer. Phys Chem Chem Phys 13:9778
75. Hansmann UHE (1997) Parallel tempering algorithm for conformational studies of biological molecules. Chem Phys Lett 281:140–150
76. Hansmann UHE, Okamoto Y (1993) Prediction of peptide conformation by multicanonical algorithm: new approach to the multiple-minima problem. J Comput Chem 14:1333–1338
77. Sugita Y, Okamoto Y (1999) Replica-exchange molecular dynamics method for protein folding. Chem Phys Lett 314:141–151
78. Götz AW, Williamson MJ, Xu D et al (2012) Routine microsecond molecular dynamics simulations with AMBER on GPUs. 1. generalized born. J Chem Theory Comput 8:1542–1555
79. Salomon-Ferrer R, Götz AW, Poole D et al (2013) Routine microsecond molecular dynamics simulations with AMBER on GPUs. 2. Explicit solvent particle mesh ewald. J Chem Theory Comput 9:3878–3888
80. Thu TTM, Co NT, Tu LA et al (2019) Aggregation rate of amyloid beta peptide is controlled by beta-content in monomeric state. J Chem Phys 150:225101
81. Minh Thu TT, Huang SH, Tu LA et al (2019) G37V mutation of Aβ42 induces a nontoxic ellipse-like aggregate: an in vitro and in silico study. Neurochem Int 129:104512
82. Nguyen HL, Thi Minh Thu T, Truong PM et al (2016) Aβ41 aggregates more like Aβ40

than like Aβ42: in silico and in vitro study. J Phys Chem B 120:7371–7379
83. Huy Pham DQ, Krupa P, Nguyen HL et al (2020) Computational model to unravel the function of amyloid-β peptides in contact with a phospholipid membrane. J Phys Chem B 124:3300–3314
84. Manna M, Mukhopadhyay C (2013) Binding, conformational transition and dimerization of amyloid-β peptide on gm1-containing ternary membrane: insights from molecular dynamics simulation. PLoS One 8:e71308
85. Brown AM, Bevan DR (2016) Molecular dynamics simulations of amyloid β-peptide (1-42): tetramer formation and membrane interactions. Biophys J 111:937–949
86. Nguyen PH, Campanera JM, Ngo ST et al (2019) Tetrameric Aβ40 and Aβ42 β-barrel structures by extensive atomistic simulations. I. In a bilayer mimicking a neuronal membrane. J Phys Chem B 123:3643–3648
87. Serra-Batiste M, Ninot-Pedrosa M, Bayoumi M et al (2016) Aβ42 assembles into specific β-barrel pore-forming oligomers in membrane-mimicking environments. Proc Natl Acad Sci U S A 113:10866–10871
88. Huy PDQ, Li MS (2014) Binding of fullerenes to amyloid beta fibrils: size matters. Phys Chem Chem Phys 16:20030–20040
89. Bednarikova Z, Huy PDQ, Mocanu MM et al (2016) Fullerenol C60(OH)16 prevents amyloid fibrillization of Aβ40-: in vitro and in silico approach. Phys Chem Chem Phys 18:18855–18867
90. Ngo ST, Li MS (2012) Curcumin binds to Aβ1-40 peptides and fibrils stronger than ibuprofen and naproxen. J Phys Chem B 116:10165–10175
91. Viet MH, Ngo ST, Lam NS et al (2011) Inhibition of aggregation of amyloid peptides by beta-sheet breaker peptides and their binding affinity. J Phys Chem B 115:7433–7446
92. Ilie IM, Caflisch A (2019) Simulation studies of amyloidogenic polypeptides and their aggregates. Chem Rev 119:6956. https://pubs.acs.org/sharingguidelines
93. Kmiecik S, Gront D, Kolinski M et al (2016) Coarse-grained protein models and their applications. Chem Rev 116:7898–7936
94. Oprzeska-Zingrebe EA, Smiatek J (2019) Some notes on the thermodynamic accuracy of coarse-grained models. Front Mol Biosci 6:87
95. Krupa P, Mozolewska MA, Wiśniewska M et al (2016) Performance of protein-structure predictions with the physics-based UNRES force field in CASP11. Bioinformatics 32:3270–3278
96. Kynast P, Derreumaux P, Strodel B (2016) Evaluation of the coarse-grained OPEP force field for protein-protein docking. BMC Biophys 9:4
97. Maisuradze G, Medina J, Kachlishvili K et al (2015) Preventing fibril formation of a protein by selective mutation. Proc Natl Acad Sci 112:13549–13554
98. Pak AJ, Voth GA (2018) Advances in coarse-grained modeling of macromolecular complexes. Curr Opin Struct Biol 52:119–126
99. Izvekov S, Voth GA (2005) A multiscale coarse-graining method for biomolecular systems. J Phys Chem B 109:2469–2473
100. Wang Y, Noid WG, Liu P et al (2009) Effective force coarse-graining. Phys Chem Chem Phys 11:2002–2015
101. Uhlig F, Zeman J, Smiatek J et al (2018) First-principles parametrization of polarizable coarse-grained force fields for ionic liquids. J Chem Theory Comput 14:1471–1486
102. Dannenhoffer-Lafage T, Voth GA (2020) Reactive coarse-grained molecular dynamics. J Chem Theory Comput 16:2541–2549
103. Rao S, Li X, Liang H (2007) Developing coarse-grained force fields for polystyrene with different chain lengths from atomistic simulation. Macromol Res 15:610–616
104. Botan V, Ustach VD, Leonhard K et al (2017) Development and application of a coarse-grained model for PNIPAM by iterative Boltzmann inversion and its combination with lattice Boltzmann hydrodynamics. J Phys Chem B 121:10394–10406
105. Davtyan A, Schafer NP, Zheng W et al (2012) AWSEM-MD: protein structure prediction using coarse-grained physical potentials and bioinformatically based local structure biasing. J Phys Chem B 116:8494–8503
106. Kmiecik S, Kolinski A (2007) Characterization of protein-folding pathways by reduced-space modeling. Proc Natl Acad Sci U S A 104:12330–12335
107. Marrink S, Risselada H (2007) The MARTINI force field: coarse grained model for biomolecular simulations. J Phys Chem B 111:7812–7824
108. Monticelli L, Kandasamy SK, Periole X et al (2008) The MARTINI coarse-grained force field: extension to proteins. J Chem Theory Comput 4:819–834
109. Derreumaux P (1999) From polypeptide sequences to structures using Monte Carlo simulations and an optimized potential. J Chem Phys 111:2301–2310

110. Maupetit J, Tuffery P, Derreumaux P (2007) A coarse-grained protein force field for folding and structure prediction. Proteins 69:394–408
111. Pasi M, Lavery R, Ceres N (2013) PaLaCe: a coarse-grain protein model for studying mechanical properties. J Chem Theory Comput 9:785–793
112. Kar P, Gopal SM, Cheng Y-M et al (2013) PRIMO: a transferable coarse-grained force field for proteins. J Chem Theory Comput 9:3769–3788
113. Darré L, MacHado MR, Dans PD et al (2010) Another coarse grain model for aqueous solvation: WAT FOUR? J Chem Theory Comput 6:3793–3807
114. Machado MR, Barrera EE, Klein F et al (2019) The SIRAH 2.0 force field: altius, fortius, citius. J Chem Theory Comput 15:2719–2733
115. Liwo A, Ołdziej S, Pincus MR et al (1997) A united-residue force field for off-lattice protein-structure simulations. I. Functional forms and parameters of long-range side-chain interaction potentials from protein crystal data. J Comput Chem 18:849–873
116. Khalili M, Liwo A, Jagielska A et al (2005) Molecular dynamics with the united-residue model of polypeptide chains. II. Langevin and Berendsen-bath dynamics and tests on model alpha-helical systems. J Phys Chem B 109:13798–13810
117. Liwo A, Baranowski M, Czaplewski C et al (2014) A unified coarse-grained model of biological macromolecules based on mean-field multipole-multipole interactions. J Mol Model 20:2306
118. Singh N, Li W (2019) Recent advances in coarse-grained models for biomolecules and their applications. Int J Mol Sci 20:3774
119. Javanainen M, Martinez-Seara H, Vattulainen I (2017) Excessive aggregation of membrane proteins in the Martini model. PLoS One 12: e0187936
120. Marrink SJ, Corradi V, Souza PCT et al (2019) Computational modeling of realistic cell membranes. Chem Rev 119:6184
121. Wu H, Wolynes PG, Papoian GA (2018) AWSEM-IDP: a coarse-grained force field for intrinsically disordered proteins. J Phys Chem B 122:11115–11125
122. Ramis R, Ortega-Castro J, Casasnovas R et al (2019) A coarse-grained molecular dynamics approach to the study of the intrinsically disordered protein α-synuclein. J Chem Inf Model 59:1458–1471
123. Kosciolek T, Buchan DWA, Jones DT (2017) Predictions of backbone dynamics in intrinsically disordered proteins using de novo fragment-based protein structure predictions. Sci Rep 7:1–12
124. Jamroz M, Orozco M, Kolinski A et al (2013) Consistent view of protein fluctuations from all-atom molecular dynamics and coarse-grained dynamics with knowledge-based force-field. J Chem Theory Comput 9:119–125
125. Berman HM (2000) The protein data bank. Nucleic Acids Res 28:235–242
126. Berggård T, Linse S, James P (2007) Methods for the detection and analysis of protein-protein interactions. Proteomics 7:2833–2842
127. Chen M, Schafer NP, Zheng W et al (2018) The associative memory, water mediated, structure and energy model (AWSEM)-Amylometer: predicting amyloid propensity and fibril topology using an optimized folding landscape model. ACS Chem Neurosci 9:1027–1039
128. Chen X, Chen M, Schafer NP et al (2020) Exploring the interplay between fibrillization and amorphous aggregation channels on the energy landscapes of tau repeat isoforms. Proc Natl Acad Sci U S A 117:4125–4130
129. Saracino GAA, Fontana F, Jekhmane S et al (2018) Elucidating self-assembling peptide aggregation via morphoscanner: a new tool for protein-peptide structural characterization. Adv Sci 5:1800471
130. Frederix PWJM, Ulijn RV, Hunt NT et al (2011) Virtual screening for dipeptide aggregation: toward predictive tools for peptide self-Assembly. J Phys Chem Lett 2:2380–2384
131. Szała B, Molski A (2019) Aggregation kinetics of short peptides: all-atom and coarse-grained molecular dynamics study. Biophys Chem 253:106219
132. Pannuzzo M, Milardi D, Raudino A et al (2013) Analytical model and multiscale simulations of Aβ peptide aggregation in lipid membranes: towards a unifying description of conformational transitions, oligomerization and membrane damage. Phys Chem Chem Phys 15:8940–8951
133. Kar P, Gopal SM, Cheng YM et al (2014) Transferring the PRIMO coarse-grained force field to the membrane environment: simulations of membrane proteins and helix-helix association. J Chem Theory Comput 10:3459–3472

134. Yu H, Han W, Ma W et al (2015) Transient β -hairpin formation in α -synuclein monomer revealed by coarse-grained molecular dynamics simulation. J Chem Phys 143:243142
135. Brodie NI, Popov KI, Petrotchenko EV et al (2019) Conformational ensemble of native α-synuclein in solution as determined by short-distance crosslinking constraint-guided discrete molecular dynamics simulations. PLoS Comput Biol 15:e1006859
136. Katyal N, Agarwal M, Sen R et al (2018) Paradoxical effect of trehalose on the aggregation of α-synuclein: expedites onset of aggregation yet reduces fibril load. ACS Chem Neurosci 9:1477–1491
137. Smit FX, Luiken JA, Bolhuis PG (2017) Primary fibril nucleation of aggregation prone tau fragments PHF6 and PHF6. J Phys Chem B 121:3250–3261
138. Cheon M, Chang I, Hall CK (2012) Influence of temperature on formation of perfect tau fragment fibrils using PRIME20/DMD simulations. Protein Sci 21:1514–1527
139. Chebaro Y, Pasquali S, Derreumaux P (2012) The coarse-grained OPEP force field for non-amyloid and amyloid proteins. J Phys Chem B 116:8741–8752
140. Sterpone F, Nguyen PH, Kalimeri M et al (2013) Importance of the ion-pair interactions in the OPEP coarse-grained force field: parametrization and validation. J Chem Theory Comput 9:4574–4584
141. Barroso Da Silva FL, Sterpone F, Derreumaux P (2019) OPEP6: a new constant-pH molecular dynamics simulation scheme with OPEP coarse-grained force field. J Chem Theory Comput 15:3875–3888
142. Kalimeri M, Derreumaux P, Sterpone F (2015) Are coarse-grained models apt to detect protein thermal stability? the case of OPEP force field. J Non-Cryst Solids 407:494–501
143. Spill YG, Pasquali S, Derreumaux P (2011) Impact of thermostats on folding and aggregation properties of peptides using the optimized potential for efficient structure prediction coarse-grained model. J Chem Theory Comput 7:1502–1510
144. Mousseau N, Derreumaux P (2005) Exploring the early steps of amyloid peptide aggregation by computers. Acc Chem Res 38:885–891
145. Song W, Wei G, Mousseau N et al (2008) Self-assembly of the β2-microglobulin NHVTLSQ peptide using a coarse-grained protein model reveals a β-barrel species. J Phys Chem B 112:4410–4418
146. Simone AD, Derreumaux P (2010) Low molecular weight oligomers of amyloid peptides display B-barrel conformations: a replica exchange molecular dynamics study in explicit solvent. J Chem Phys 132:165103
147. Ngo ST, Nguyen PH, Derreumaux P (2020) Stability of Aβ11-40 trimers with parallel and antiparallel β-sheet organizations in a membrane-mimicking environment by replica exchange molecular dynamics simulation. J Phys Chem B 124:617–626
148. Chiricotto M, Melchionna S, Derreumaux P et al (2019) Multiscale aggregation of the amyloid Aβ 16-22 peptide: from disordered coagulation and lateral branching to amorphous prefibrils. J Phys Chem Lett 10:1594–1599
149. Sterpone F, Derreumaux P, Melchionna S (2015) Protein simulations in fluids: coupling the OPEP coarse-grained force field with hydrodynamics. J Chem Theory Comput 11:1843–1853
150. Lee J, Liwo A, Scheraga HA (1999) Energy-based de novo protein folding by conformational space annealing and an off-lattice united-residue force field: application to the 10-55 fragment of staphylococcal protein A and to apo calbindin D9K. Proc Natl Acad Sci U S A 96:2025–2030
151. He Y, Mozolewska MA, Krupa P et al (2013) Lessons from application of the UNRES force field to predictions of structures of CASP10 targets. Proc Natl Acad Sci U S A 110:14936
152. Lensink MF, Brysbaert G, Nadzirin N et al (2019) Blind prediction of homo- and hetero-protein complexes: the CASP13-CAPRI experiment. Proteins 87:1200–1221
153. Rojas AV, Liwo A, Scheraga HA (2007) Molecular dynamics with the United-residue force field: ab initio folding simulations of multichain proteins. J Phys Chem B 111:293–309
154. Yaşar F, Sieradzan AK, Hansmann UHE (2014) Folding and self-assembly of a small heterotetramer. J Chem Phys 140:105103
155. Nguyen HL, Krupa P, Hai NM et al (2019) Structure and physicochemical properties of the Aβ42 tetramer: multiscale molecular dynamics simulations. J Phys Chem B 123:7253–7269
156. Khoury GA, Liwo A, Khatib F et al (2014) WeFold: a coopetition for protein structure prediction. Proteins 82:1850–1868
157. Karczyńska AS, Mozolewska MA, Krupa P et al (2017) Prediction of protein structure with the coarse-grained UNRES force field assisted by small X-ray scattering data and

knowledge-based information. Proteins Struct Funct Bioinf 86:228

158. Krupa P, Mozolewska MA, Joo K et al (2015) Prediction of protein structure by template-based modeling combined with the UNRES force field. J Chem Inf Model 55:1271–1281
159. Mozolewska MA, Krupa P, Zaborowski B et al (2016) Use of restraints from consensus fragments of multiple server models to enhance protein-structure prediction capability of the UNRES force field. J Chem Inf Model 56:2263–2279
160. Rojas A, Liwo A, Browne D et al (2010) Mechanism of fiber assembly: treatment of Aβ peptide aggregation with a coarse-grained united-residue force field. J Mol Biol 404:537–552
161. Rojas A, Maisuradze N, Kachlishvili K et al (2017) Elucidating important sites and the mechanism for amyloid fibril formation by coarse-grained molecular dynamics. ACS Chem Neurosci 8:201–209
162. Rojas AV, Liwo A, Scheraga HA (2011) A study of the α-helical intermediate preceding the aggregation of the amino-terminal fragment of the β amyloid peptide (Aβ 1-28). J Phys Chem B 115:12978–12983
163. Rojas AV, Maisuradze GG, Scheraga HA (2018) Dependence of the formation of Tau and Aβ peptide mixed aggregates on the secondary structure of the N-terminal region of Aβ. J Phys Chem B 122:7049–7056
164. Barz B, Liao Q, Strodel B (2018) Pathways of amyloid-β aggregation depend on oligomer shape. J Am Chem Soc 140:319–327
165. Vácha R, Frenkel D (2011) Relation between molecular shape and the morphology of self-assembling aggregates: a simulation study. Biophys J 101:1432–1439
166. Bieler NS, Knowles TPJ, Frenkel D et al (2012) Connecting macroscopic observables and microscopic assembly events in amyloid formation using coarse grained simulations. PLoS Comput Biol 8:e1002692
167. Šarić A, Chebaro YC, Knowles TPJ et al (2014) Crucial role of nonspecific interactions in amyloid nucleation. Proc Natl Acad Sci 111:17869
168. Michaels TCT, Liu LX, Curk S et al (2018) Reaction rate theory for supramolecular kinetics: application to protein aggregation. Mol Phys 116:3055–3065
169. Šarić A, Buell AK, Meisl G et al (2016) Physical determinants of the self-replication of protein fibrils. Nat Phys 12:874–880
170. Vácha R, Linse S, Lund M (2014) Surface effects on aggregation kinetics of amyloidogenic peptides. J Am Chem Soc 136:11776–11782
171. Barz B, Urbanc B (2014) Minimal model of self-assembly: emergence of diversity and complexity. J Phys Chem B 118:3761–3770
172. Hoang TX, Trovato A, Seno F et al (2004) Geometry and symmetry presculpt the free-energy landscape of proteins. Proc Natl Acad Sci U S A 101:7960–7964
173. Auer S, Dobson CM, Vendruscolo M (2007) Characterization of the nucleation barriers for protein aggregation and amyloid formation. HFSP J 1:137–146
174. Auer S, Meersman F, Dobson CM et al (2008) A generic mechanism of emergence of amyloid protofilaments from disordered oligomeric aggregates. PLoS Comput Biol 4: e1000222
175. Hung NB, Le D-M, Hoang TX (2017) Sequence dependent aggregation of peptides and fibril formation. J Chem Phys 147:105102
176. Mioduszewski Ł, Cieplak M (2018) Disordered peptide chains in an α-C-based coarse-grained model. Phys Chem Chem Phys 20:19057–19070
177. Mioduszewski Ł, Cieplak M (2020) Protein droplets in systems of disordered homopeptides and the amyloid glass phase. Phys Chem Chem Phys 22:15592–15599
178. Mioduszewski Ł, Różycki B, Cieplak M (2020) Pseudo-improper-dihedral model for intrinsically disordered proteins. J Chem Theory Comput 16:4726–4733
179. Ilie IM, Otter WK, Briels WJ (2016) A coarse grained protein model with internal degrees of freedom. Application to α-synuclein aggregation. J Chem Phys 144:85103
180. Ilie IM, Otter WK, Briels WJ (2017) The attachment of α-synuclein to a fiber: a coarse-grain approach. J Chem Phys 146:115102
181. Pellarin R, Caflisch A (2006) Interpreting the aggregation kinetics of amyloid peptides. J Mol Biol 360:882–892
182. Pellarin R, Guarnera E, Caflisch A (2007) Pathways and intermediates of amyloid fibril formation. J Mol Biol 374:917–924
183. Pellarin R, Schuetz P, Guarnera E et al (2010) Amyloid fibril polymorphism is under kinetic control. J Am Chem Soc 132:14960–14970
184. Friedman R, Caflisch A (2011) Surfactant effects on amyloid aggregation kinetics. J Mol Biol 414:303–312
185. Magno A, Caflisch A, Pellarin R (2010) Crowding effects on amyloid aggregation kinetics. J Phys Chem Lett 1:3027–3032

186. Friedman R, Pellarin R, Caflisch A (2009) Amyloid aggregation on lipid bilayers and its impact on membrane permeability. J Mol Biol 387:407–415
187. Bellesia G, Shea J-E (2007) Self-assembly of β-sheet forming peptides into chiral fibrillar aggregates. J Chem Phys 126:245104
188. Bellesia G, Shea J-E (2009) Diversity of kinetic pathways in amyloid fibril formation. J Chem Phys 131:111102
189. Morriss-Andrews A, Brown FLH, Shea J-E (2014) A coarse-grained model for peptide aggregation on a membrane surface. J Phys Chem B 118:8420–8432
190. Li MS, Klimov DK, Straub JE et al (2008) Probing the mechanisms of fibril formation using lattice models. J Chem Phys 129:175101
191. Li MS, Co NT, Reddy G et al (2010) Factors governing fibrillogenesis of polypeptide chains revealed by lattice models. Phys Rev Lett 105:218101
192. Co NT, Hu C-K, Li MS (2013) Dual effect of crowders on fibrillation kinetics of polypeptide chains revealed by lattice models. J Chem Phys 138:185101
193. Co NT, Li MS (2012) New method for determining size of critical nucleus of fibril formation of polypeptide chains. J Chem Phys 137:95101
194. Kouza M, Co NT, Nguyen PH et al (2015) Preformed template fluctuations promote fibril formation: insights from lattice and all-atom models. J Chem Phys 142:145104
195. Kouza M, Co NT, Li MS et al (2018) Kinetics and mechanical stability of the fibril state control fibril formation time of polypeptide chains: a computational study. J Chem Phys 148:215106
196. Irbäck A, Jónsson S, Linnemann N et al (2013) Aggregate geometry in amyloid fibril nucleation. Phys Rev Lett 110:058101
197. Zhang J, Muthukumar M (2009) Simulations of nucleation and elongation of amyloid fibrils. J Chem Phys 130:35102
198. Abeln S, Vendruscolo M, Dobson CM et al (2014) A simple lattice model that captures protein folding, aggregation and amyloid formation. PLoS One 9:e85185
199. Ni R, Abeln S, Schor M et al (2013) Interplay between folding and assembly of fibril-forming polypeptides. Phys Rev Lett 111:58101
200. Tran TT, Nguyen PH, Derreumaux P (2016) Lattice model for amyloid peptides: OPEP force field parametrization and applications to the nucleus size of Alzheimer's peptides. J Chem Phys 144:205103
201. Chiti F, Stefani M, Taddei N et al (2003) Rationalization of the effects of mutations on peptide andprotein aggregation rates. Nature 424:805–808
202. Bowerman CJ, Ryan DM, Nissan DA et al (2009) The effect of increasing hydrophobicity on the self-assembly of amphipathic β-sheet peptides. Mol BioSyst 5:1058–1069
203. Fowler DM, Koulov AV, Alory-Jost C et al (2005) Functional amyloid formation within mammalian tissue. PLoS Biol 4:e6
204. Ferrone F (1999) Analysis of protein aggregation kinetics. Methods Enzymol 309:256–274
205. Asakura S, Oosawa F (1954) On interaction between two bodies immersed in a solution of macromolecules. J Chem Phys 22:1255–1256
206. Zhou H-X, Rivas G, Minton AP (2008) Macromolecular crowding and confinement: biochemical, biophysical, and potential physiological consequences. Annu Rev Biophys 37:375–397
207. Obrien EP, Straub JE, Brooks BR et al (2011) Influence of nanoparticle size and shape on oligomer formation of an amyloidogenic peptide. J Phys Chem Lett 2:1171–1177
208. Wu WH, Sun X, Yu YP et al (2008) TiO2 nanoparticles promote β-amyloid fibrillation in vitro. Biochem Biophys Res Commun 373:315–318
209. Cabaleiro-Lago C, Quinlan-Pluck F, Lynch I et al (2010) Dual effect of amino modified polystyrene nanoparticles on amyloid β protein fibrillation. ACS Chem Neurosci 1:279–287
210. Co NT, Lan PD, Quoc Huy PD et al (2020) Heat-induced degradation of fibrils: exponential vs logistic kinetics. J Chem Phys 152:115101
211. Yu I, Mori T, Ando T et al (2016) Biomolecular interactions modulate macromolecular structure and dynamics in atomistic model of a bacterial cytoplasm. elife 5:e19274
212. Harada R, Tochio N, Kigawa T et al (2013) Reduced native state stability in crowded cellular environment due to protein-protein interactions. J Am Chem Soc 135:3696–3701
213. Ignatova Z, Krishnan B, Bombardier JP et al (2007) From the test tube to the cell: exploring the folding and aggregation of a β-clam protein. Biopolymers 88:157–163
214. Zhou HX (2013) Influence of crowded cellular environments on protein folding, binding, and oligomerization: biological consequences

and potentials of atomistic modeling. FEBS Lett 587:1053–1061

215. Ng W (2015) What drives computational chemistry forward: theory or computational power? Preprint
216. Aldeghi M, Biggin PC (2017) Advances in molecular simulation. In: Comprehensive medicinal chemistry III. Elsevier Inc, Amsterdam, pp 14–33
217. Ren P, Ponder JW (2002) Consistent treatment of inter- and intramolecular polarization in molecular mechanics calculations. J Comput Chem 23:1497–1506
218. Ponder JW, Wu C, Ren P et al (2010) Current status of the AMOEBA polarizable force field. J Phys Chem B 114:2549–2564
219. Faller P, Hureau C, Penna GL (2014) Metal ions and intrinsically disordered proteins and peptides: from Cu/Zn amyloid-β to general principles. Acc Chem Res 47:2252–2259
220. Gkeka P, Stoltz G, Barati Farimani A et al (2020) Machine learning force fields and coarse-grained variables in molecular dynamics: application to materials and biological systems. J Chem Theory Comput 16:4775